

Article

Displacement Sensing of an Active String Actuator Using a Step-Index Multimode Optical Fiber Sensor [†]

Weihang Tian, Shuichi Wakimoto * , Takefumi Kanda and Daisuke Yamaguchi 

Graduate School of Natural Science and Technology, Okayama University, Okayama 700-8530, Japan; pd339tfj@s.okayama-u.ac.jp (W.T.); kanda-t@okayama-u.ac.jp (T.K.); yamaguchi20@okayama-u.ac.jp (D.Y.)

* Correspondence: wakimoto@okayama-u.ac.jp

[†] The paper is an extension of conference: Tian, W.; Wakimoto, S.; Nagaoka, K.; Yoshimoto, Y.; Kanda, T.; Yamaguchi, D. Displacement Sensing of an Active String Actuator by an Optical Fiber. In Proceedings of the 8th International Electronic Conference on Sensors and Application, Online, 1–15 November 2021.

Abstract: A thin McKibben artificial muscle is a pneumatic actuator with an outer diameter of only 1.8 mm. We fabricated a string-shaped actuator called an “active string actuator,” which achieves a high contractile displacement by accumulating thin McKibben artificial muscles. To control the displacement, the length of the active string actuator should be estimated. However, this is difficult because bulky and rigid sensors are unsuitable for the sensor element of the active string actuator. Therefore, in this study, we propose a new sensing method for estimating the length of an active string actuator. The proposed sensing system is simple and comprises only three components: a step-index multimode optical fiber, a light emitter, and a light receiver. A step-index multimode optical fiber was combined with the active string actuator, and the length was estimated from the change in the amount of light propagating in the optical fiber when the active string actuator was driven. Fundamental experiments were conducted in this study, and the results demonstrated that the optical fiber sensor value changed with the actuator length. This suggests that it is possible to estimate the displacement of an active string actuator using an optical fiber sensor.

Keywords: thin artificial muscle; active string actuator; step-index multimode optical fiber; displacement sensing



Citation: Tian, W.; Wakimoto, S.; Kanda, T.; Yamaguchi, D.

Displacement Sensing of an Active String Actuator Using a Step-Index Multimode Optical Fiber Sensor.

Sensors **2022**, *22*, 3232. <https://doi.org/10.3390/s22093232>

Academic Editors: Stefano Mariani, Alberto Vallan and Stefan Bosse

Received: 23 March 2022

Accepted: 21 April 2022

Published: 22 April 2022

Publisher's Note: MDPI stays neutral with regard to jurisdictional claims in published maps and institutional affiliations.



Copyright: © 2022 by the authors. Licensee MDPI, Basel, Switzerland. This article is an open access article distributed under the terms and conditions of the Creative Commons Attribution (CC BY) license (<https://creativecommons.org/licenses/by/4.0/>).

1. Introduction

The McKibben artificial muscle is a pneumatic actuator developed in the 1950s [1]. The artificial muscle contracts axially and expands radially. Contraction displacement is generally utilized as the mechanical output. It has a simple structure consisting of a rubber tube and sleeve fiber and is characterized by good human compatibility and a high power-to-weight ratio. In recent years, general-purpose power-assist and rehabilitation devices that incorporate McKibben artificial muscles have become commercially available [2,3].

One of the authors of this paper developed a thin McKibben artificial muscle (hereinafter referred to as a thin artificial muscle) with an outer diameter of only 1.8 mm. By contrast, the outer diameter of a commercially available McKibben artificial muscle is between 10 mm and several tens of millimeters. The outer diameter of the developed thin artificial muscle is only 1.8 mm, making it more compliant than conventional McKibben artificial muscles. Therefore, it is possible to consider it to be composed of fibers and accumulate them in the form of strings and cloths to realize accumulated structures with softness as well as high contractility and force [4–8]. They are not only applied to power-assist and rehabilitation devices, but also to musculoskeletal mechanisms that mimic the redundant drive mechanism of the human body and robot arms with multiple degrees of freedom for contraction, bending, and twisting movements [9–13].

In a previous study, we fabricated a string-shaped actuator called an “active string actuator” by accumulating thin artificial muscles using a string production process, and it

was confirmed that the generated force and contraction ratio were improved [14]. To control the displacement, it is necessary to sense the length of the actuator. However, conventional sensors such as potentiometers or encoders are not suitable for the sensor elements of the active string actuator because they are bulky and rigid. For instance, when the active string actuator is applied to a power-assist device, conventional sensors can impede user movements owing to their weight and rigidity. Therefore, an appropriate displacement sensing method that agrees with the future of active string actuators is required so that the advantages of the actuator are retained.

Several studies have been conducted to sense the displacement of “soft” actuators such as the active string actuator. The sensors of electrical resistance types, conductive rubber sensors [15], and the liquid conductor sensors (eutectic gallium indium, eGaIn) [16] have been applied to soft actuators. Functional fibers such as sleeve fibers, which are part of the McKibben artificial muscle, can be used to estimate the displacement of the artificial muscle based on the change in the inductance [17] or capacitance [18]. In addition, Hall effect sensors [19], optical sensors [20,21], and ultrasonic sensors [22] have been used to measure the displacement of artificial muscles. In many sensing methods, the sensor itself has a complex structure that is difficult to fabricate and its integration in the actuator requires a complex procedure. Moreover, using a rigid sensor in the drive unit of the actuator may compromise the flexibility of the soft actuator [19–22].

In this study, we propose a new sensing application for estimating the displacement of an active string actuator while avoiding the aforementioned problems. A step-index multimode optical fiber was integrated in the active string actuator, and the length was estimated based on the change in the amount of light propagating in the optical fiber when the active string actuator was driven. The advantages of this sensing application are as follows:

1. Simple structure: The sensing system comprises only three components, namely, an optical fiber, a light emitter, and a light receiver. Almost all of the components are commercially available, making them inexpensive and easy to manufacture.
2. Flexible: The light emitter and receiver are located outside the drive unit, and the optical fiber located in the drive unit is flexible and thin.

We believe that the active string actuator with the optical fiber sensor that we have developed will facilitate the development of rehabilitation equipment and lead to the development of safer and more effective equipment due to its flexibility and displacement estimation capabilities. Furthermore, it will be useful in a wide variety of applications where soft robotics abilities are required.

In this paper, the structure and driving principle of an active string actuator are first introduced. Then, the sensing principle of the proposed optical fiber sensor and its integration in the active string actuator are explained, and the experimental system developed to evaluate the constructed sensor is presented in Section 2. The actuation and sensing characteristics of the active string actuator with the optical fiber sensor are described in Section 3, and the conclusions and future work are presented in Section 4.

2. Materials and Methods

2.1. Thin Artificial Muscles and Active String Actuator

An active string actuator was realized by accumulating thin artificial muscles in a round string structure. Figure 1 shows the appearance and structure of the thin artificial muscle. It has an outer diameter of 1.8 mm and consists of an inner silicone rubber tube and outer sleeve braiding of 24 fibers.

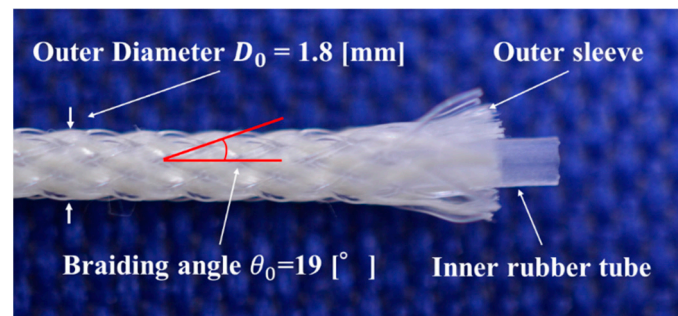


Figure 1. Appearance and structure of the thin artificial muscle.

The theoretical construction force F of the McKibben artificial muscle is calculated using the equation proposed by Schulte [23,24] as follows:

$$F = \frac{\pi}{4} D_0^2 P \left(\frac{1}{\sin \theta_0} \right)^2 \{ 3(1 - \varepsilon)^2 \cos^2 \theta_0 - 1 \}, \quad (1)$$

where D_0 is the initial diameter of the rubber tube, P is the applied pressure, θ_0 is the initial braiding angle of the sleeve, and ε is the contraction ratio. Equation (1) indicates that the construction force F depends on the initial braiding angle θ_0 . Additionally, it is defined as half of the angle between the fibers of the sleeve, as shown in Figure 1. The braiding angle of the thin artificial muscles used in this study is 19° .

Eight thin artificial muscles were assembled into a string shape using a string production process. One side was sealed and the other side was connected to an acrylic pipe resembling an air supply tube, as shown in Figure 2. The eight artificial muscles were pressurized together by applying pneumatic pressure to the air supply tube. In this study, the actuator made using this approach is called an “active string actuator.” Figure 3 the condition shows the structure of the active string actuator under the application of a pneumatic pressure of 0.3 MPa. Compared with the initial condition shown in Figure 2, the actuator contracts axially.

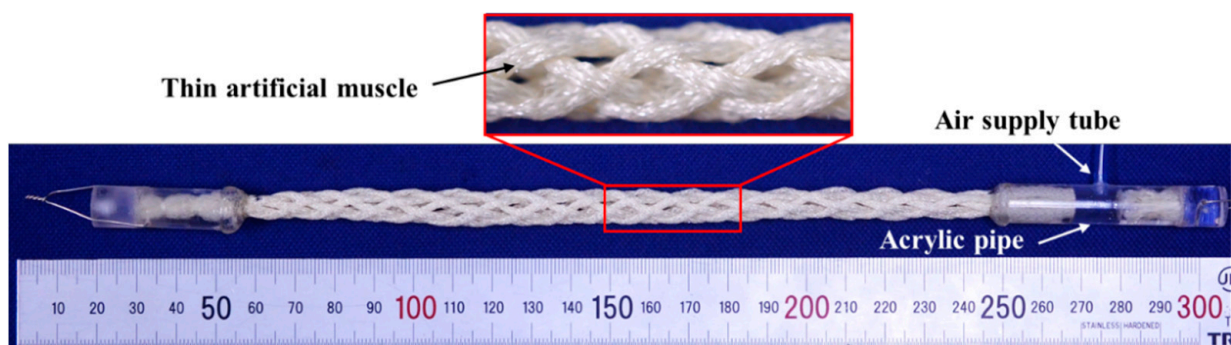


Figure 2. Appearance and structure of the active string actuator.

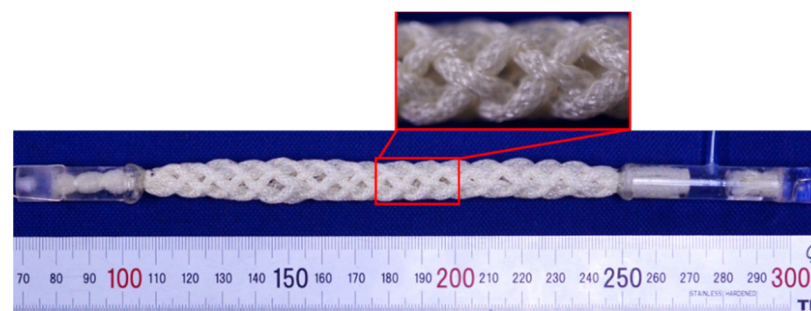


Figure 3. Active string actuator with air pressure of 0.3 MPa.

When pneumatic pressure is applied to the thin artificial muscle, it expands in the radial direction and contracts in the axial direction, as shown in Figure 4a, and the total length of the active string actuator decreases. When the artificial muscles were assembled in the form of a braided string, the crossing angle of the thin artificial muscles increased with the application of air pressure, as shown in Figure 4b, which caused the active string actuator to contract, as it functions similar to the pantograph mechanism. The contraction of the active string actuator is achieved by combining the contraction of the thin artificial muscle and the pantograph mechanism, such that the entire active string actuator significantly contracts in the axial direction.

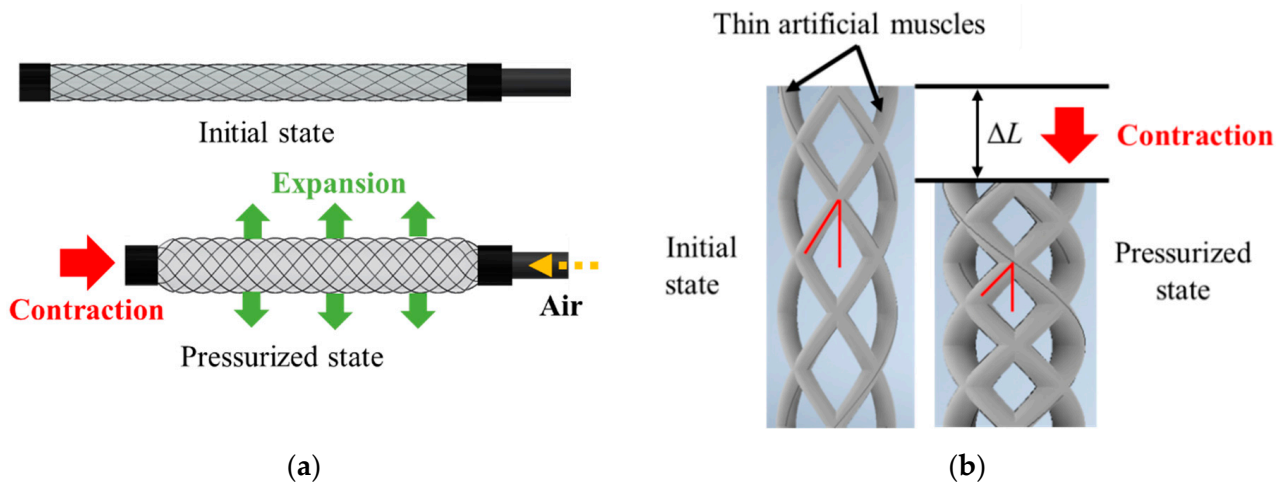


Figure 4. Contraction of the active string actuator: (a) contraction of the thin artificial muscle; (b) contraction using the pantograph mechanism.

2.2. Step-Index Multimode Optical Fiber Sensor

A step-index multimode optical fiber (GCK-20E 0.5, MITUBISHI CHEMICAL) was used in this study. The optical fiber has the advantages of low cost, flexibility, bending resistance, and small diameter, and it can be easily integrated in active string actuators. The method for integrating optical fibers in the active string actuator is described in Section 2.3.

The outer diameter of the step-index multimode optical fiber used in this study is 0.5 mm, and the fiber comprises two layers: a core layer and cladding layer. The refractive index of the cladding layer is lower than that of the core layer. When the light incident angle θ_{in} is greater than the critical angle θ_{lim} , the incident light in the optical fiber propagates through the core layer with repeated total reflection, as depicted in Figure 5a. However, when the optical fiber is bent, the incident angle θ_{in} becomes smaller than the critical angle θ_{lim} , and the light begins to leak out as shown in Figure 5b. This phenomenon is known as the bending loss of light in the optical fiber. Consequently, as the radius of curvature of the optical fiber decreases, the amount of light propagating in the optical fiber decreases accordingly.

To use a step-index multimode optical fiber as a sensor, a light emitter is required at one end and a light receiver at the other end to measure the light intensity. As shown in Figure 6, we used a white LED (C503D-WAN-CCbEb151, Cree LED) as the light emitter and a photo IC diode (S13948-01SB, Hamamatsu Photonics) as the light receiver. A photo IC diode is an electronic component that generates an electrical current output in proportion to the amount of light incident on it. In this study, the photo IC diode was connected in series to a resistor, and the voltage output of the resistor was used as the sensor voltage.

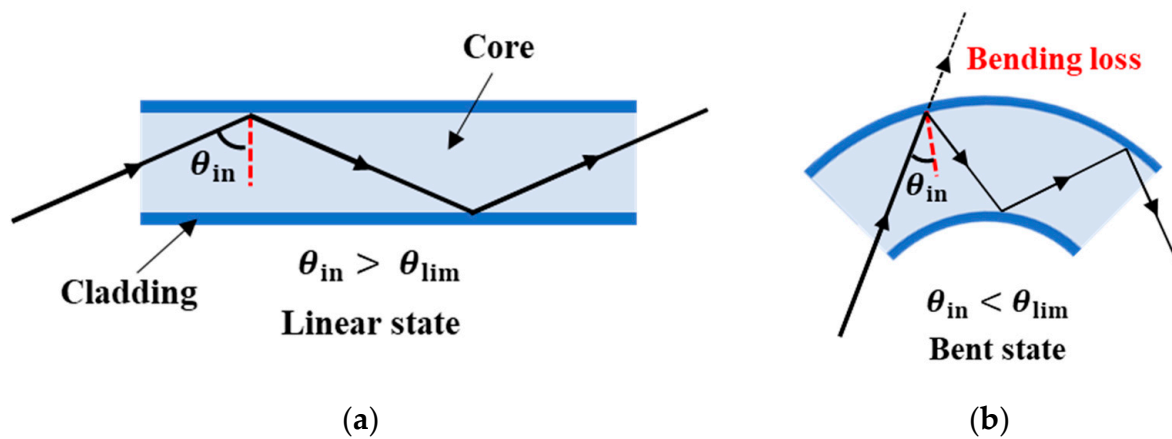


Figure 5. Bending loss of the optical fiber: (a) linear state; (b) bent state.

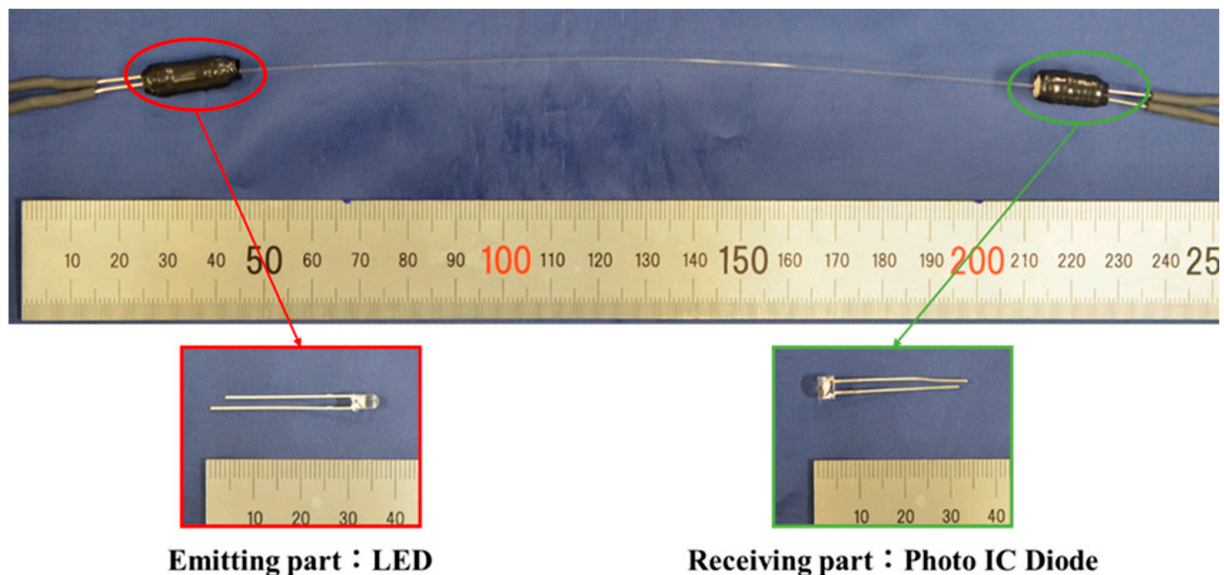


Figure 6. Appearance and structure of the step-index multimode optical fiber sensor.

As shown in Figure 7, rubber parts with small openings of 0.5 mm in diameter were fabricated, and electronic components (LED for the light-emitting part and photo IC diode for the light-receiving part) are sandwiched by them. One of the rubber parts had an opening for inserting the optical fiber, and the other had two small openings for electrical wiring. They were covered with a thin aluminum film and heat-shrinkable tubes to prevent penetration of external light and light leakage from the components.

Electronic component
(LED for Emitting part and Photo IC Diode for receiving part)

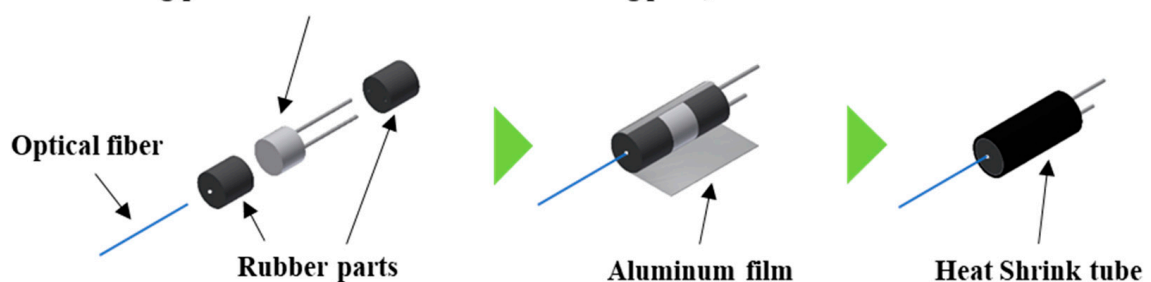


Figure 7. Structure of the emitting and receiving parts.

We measured the change in the sensor output corresponding to the curvature of a single optical fiber. Figure 8 illustrates the experimental setup. We connected the light emitter to one end of the optical fiber and the light receiver to the other end. With the optical fiber curving, the radius of curvature of the optical fiber and the sensor output, which is the voltage of the receiving part, were recorded. Figure 9 shows the relationship between the radius of curvature of the optical fiber and the sensor output. Although the sensor output changed corresponding to the radius of curvature with a range lower than 50 mm, no change was observed in the sensor output for a radius of curvature greater than 50 mm. The reason for this sensor dead zone is that the light incident angle θ_{in} is smaller than θ_{lim} when the bending extent is low.

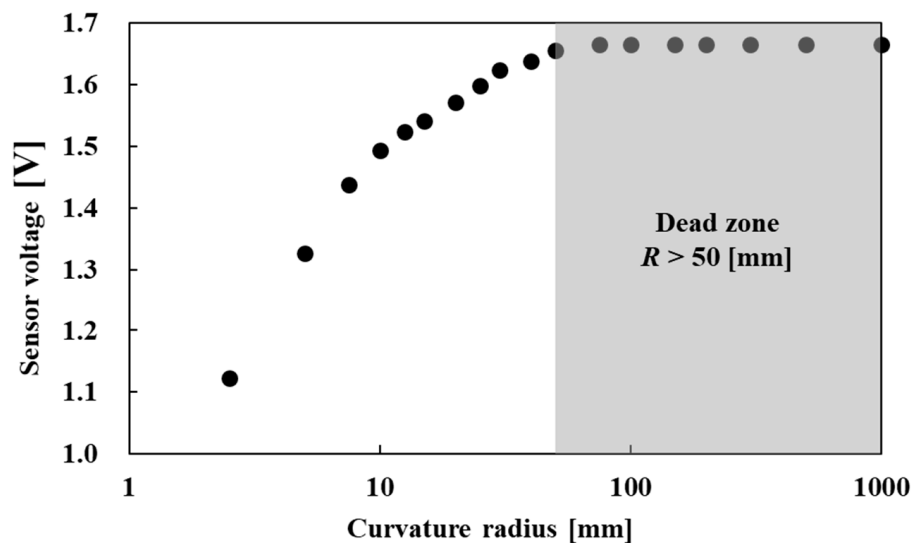


Figure 8. Relationship between the curvature radius and sensor voltage.

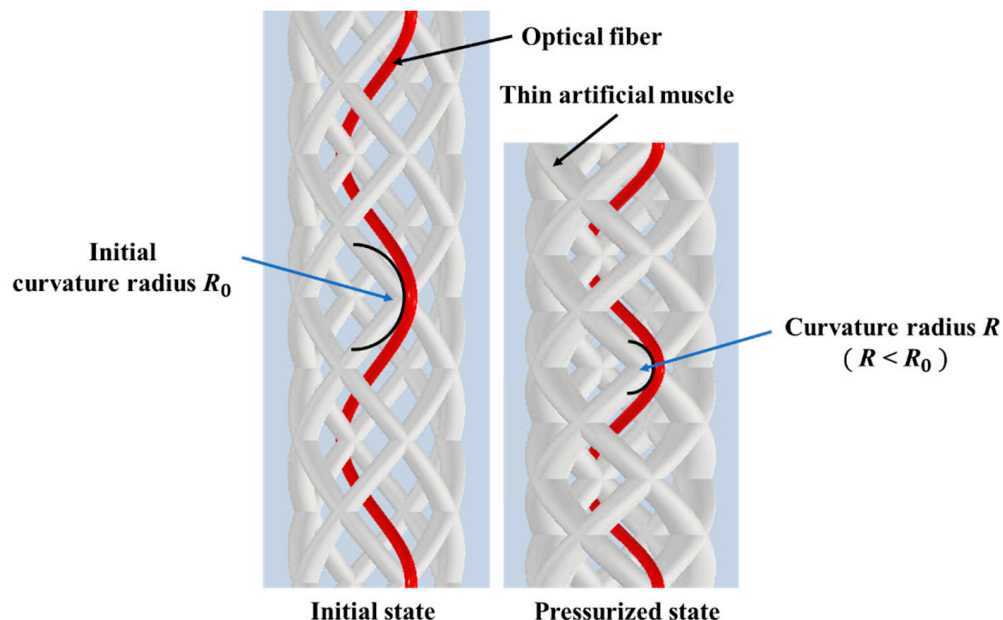


Figure 9. Integrating the optical fiber sensor in the active string actuator.

2.3. Active String Actuator with Optical Fiber Sensor

The optical fiber sensor itself uses an already known phenomenon, the bending loss, but as a means of estimating the displacement of an active string actuator has not been available before, it is new as an actuator-sensor system.

The optical fiber was integrated in the active string actuator in a wave-like form by sewing between braided thin artificial muscles, as depicted in Figure 9. When the active string actuator contracted owing to air pressure, the waveform of the optical fiber changed with a change in the radius of curvature. Consequently, the amount of light propagating in the optical fiber decreased. The length of the active string actuator can be estimated by measuring the amount of light using a photo IC diode.

Figure 10 shows the appearance of the active string actuator with the optical fiber sensor. The black dashed line represents the optical fiber embedded in braided thin artificial muscles.

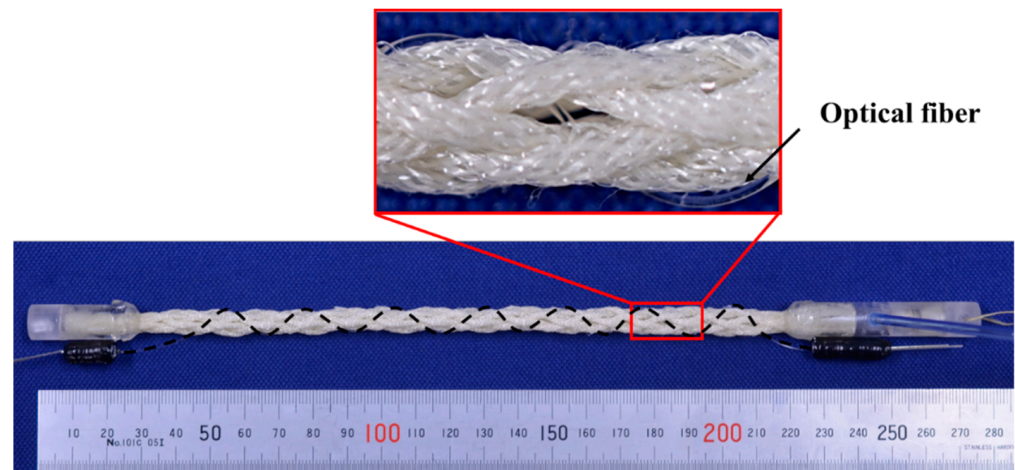


Figure 10. Appearance of the active string actuator that integrates the optical fiber sensor in a wave-like pattern.

Figure 11 shows the optical fiber in the initial state and contraction state, wherein air pressure was applied. The radius of curvature of the optical fiber decreased with the contraction of the active string actuator.

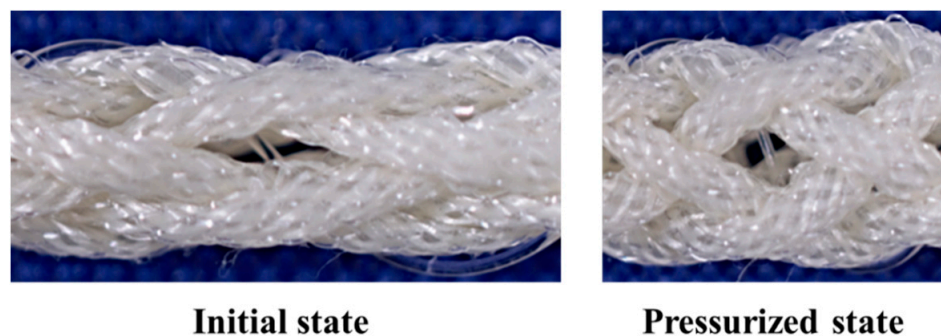


Figure 11. Enlarged view of the active string actuator.

2.4. Experimental System

Figure 12 illustrates the experimental setup for measuring the basic characteristics of the active string actuator with the optical fiber. To evaluate the optical fiber sensor, we used a linear potentiometer (LP-100FJ-5K, MIDORI PRECISIONS) to measure the actual length of the active string actuator. The signal from the linear potentiometer and photo IC diode was read using a PC. Additionally, an electropneumatic regulator (EVT500-0-E2-3, CKD) was used to apply air pressure proportional to the output signal from the PC to the active string actuator.

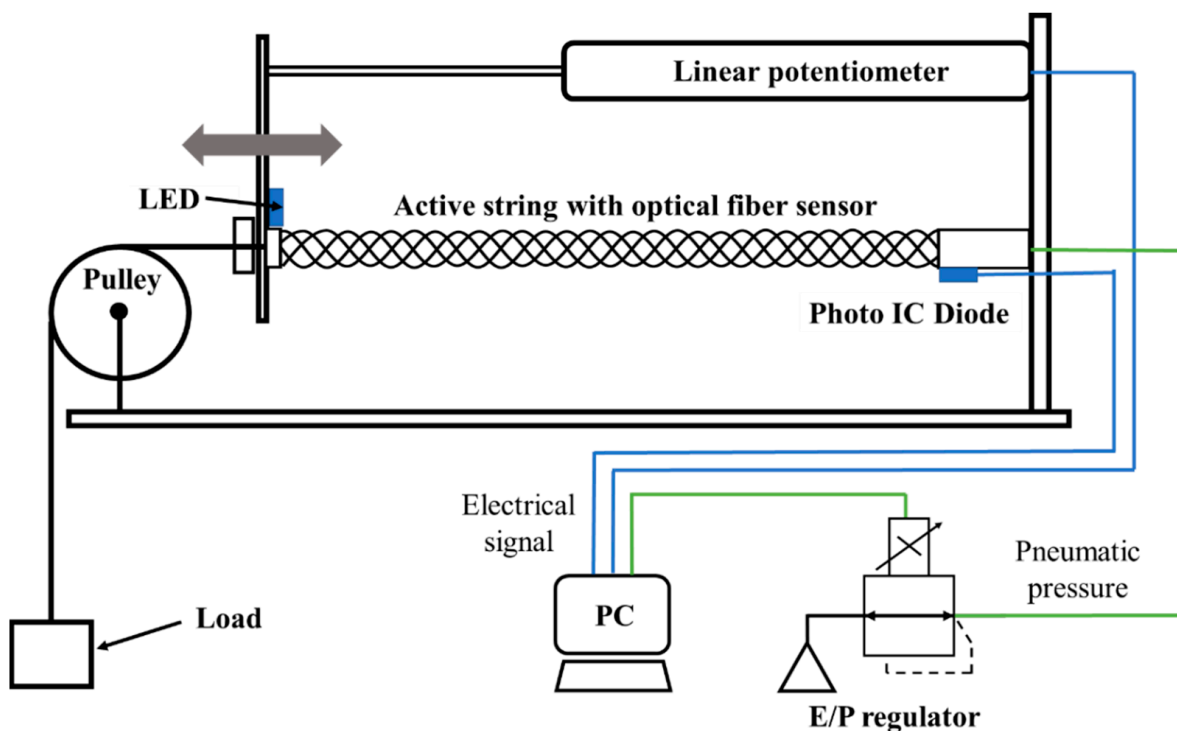


Figure 12. Schematic of the measurement system.

3. Results and Discussion

3.1. Contraction Characteristics of the Active String Actuator

The contraction capabilities of the active string actuator with and without the optical fiber were measured to examine the effect of the optical fiber sensor on the actuation characteristics of the active string actuator. In the measurement experiments, the load was set to 1.0 N to ensure that the active string actuator was taut and driven stably. Air pressure was continuously applied to the active string actuator from 0.0 MPa to 0.3 MPa (with and without the optical fiber) and then reduced to 0.0 MPa.

Figure 13 shows the contraction characteristics of the active string actuator with and without the optical fiber. The red and black lines in the figure indicate these characteristics. This can be observed from the figure in which hysteresis occurs. The generation of hysteresis in the driving characteristics of the accumulated structure of thin artificial muscles is a general phenomenon and has been reported [6,25]. There are two main reasons for this: the effect of the original hysteresis of the thin artificial muscles and the generation of friction force between the thin artificial muscles.

At an applied pressure of 0.3 MPa, the contraction of the active string actuator was 34.1 mm, whereas that of the active string actuator with the optical fiber was 32.6 mm. By embedding the optical fiber, the contraction was reduced by 1.5 mm of the absolute value (this represents 4.5% of the maximum contraction of the active string actuator without the optical fiber). The stiffness of the optical fiber (although it is not a rigid material) and contact friction between the optical fiber and thin artificial muscles inhibit the contraction of the active string actuator. The rate of contraction can be reduced by increasing the composite pitch and using low-stiffness optical fibers (thin optical fibers).

The reduction rate can be decreased using an optical fiber that is thinner than the one used in this study and by optimizing the pitch of the wave pattern when it is combined.

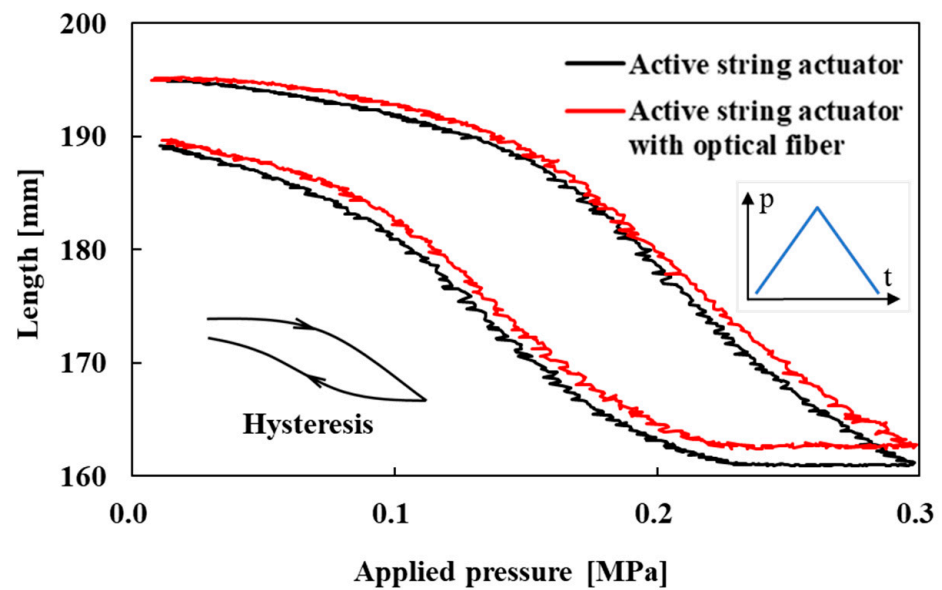


Figure 13. Contraction characteristics of the active string actuator with and without the optical fiber sensor.

3.2. Characteristics of the Active String Actuator with the Optical Fiber Sensor

The correlation between the sensor voltage and the length of the active string actuator with the optical fiber sensor was investigated. In the experiment, the load was set to 1.0 N as in the experiment in Section 3.1. Pneumatic pressure was repeatedly applied to the active string actuator with the optical fiber sensor from 0.0 MPa to 0.3 MPa for 30 s and then reduced to 0.0 MPa for 30 s. To test the robustness of the sensor, the pressure was reduced to 0.0 MPa and held for 60 s. The changes in the length of the active string actuator and the voltage output of the optical fiber sensor over time are shown in Figure 14.

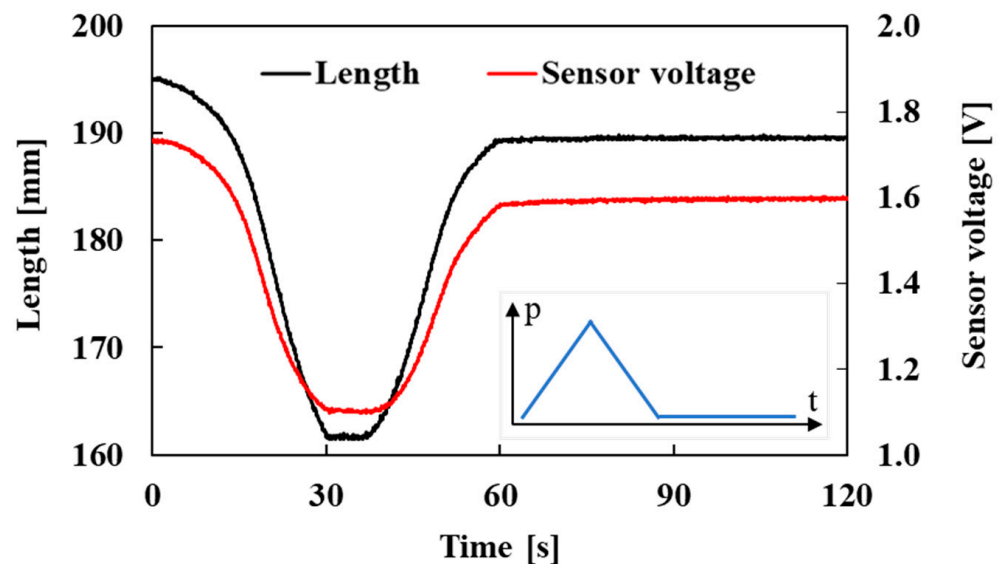


Figure 14. Length and sensor voltage variation with respect to time (pneumatic pressure: 0.0 MPa \rightarrow 0.3 MPa \rightarrow 0.0 MPa, then held until 120 s).

Figure 14 shows the change in the sensor voltage and length; the red and black lines indicate these characteristics. When the air pressure was held at 0.0 MPa (60 s to 120 s), the sensor output was stable.

The relationship between the length of the active string actuator and the voltage output of the optical fiber sensor is shown in Figure 15. The hysteresis was slight, and

the sensor voltage correlated with the length of the active string actuator over the entire driving range. Since the optical fiber was not fixed to thin artificial muscles, this was the cause of the hysteresis.

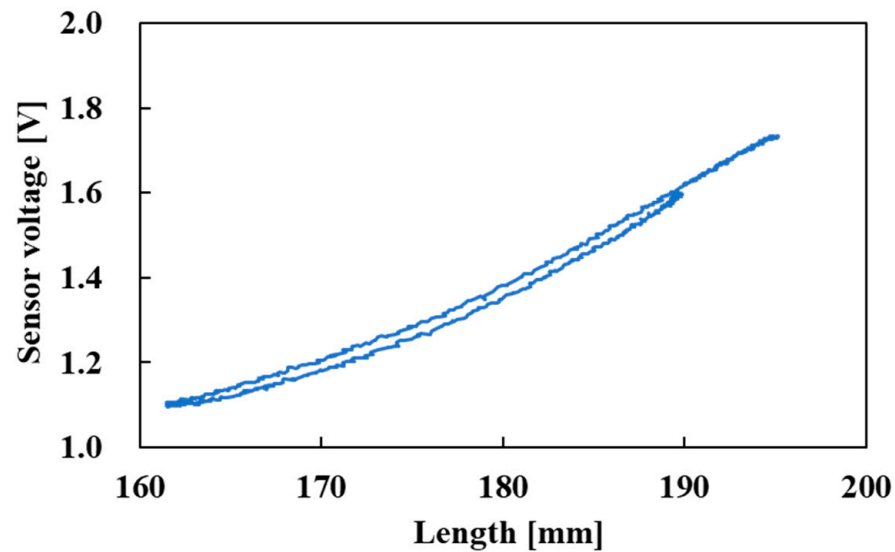


Figure 15. Relationship between length and sensor voltage (pneumatic pressure: 0.0 MPa \rightarrow 0.3 MPa \rightarrow 0.0 MPa, then held until 120 s).

In addition, to check the reproducibility of the sensor output, pneumatic pressure was repeatedly applied to the active string actuator with the optical fiber sensor five times, rising from 0.0 MPa to 0.3 MPa and falling back to 0.0 MPa. The changes in the length of the active string actuator and the voltage output of the optical fiber sensor over time are shown in Figure 16. Notably, the electrical signal from the PC in Figure 12 is a triangular waveform; however, the actuator length changed sinusoidally, corresponding to the pneumatic pressure because of its nonlinearity.

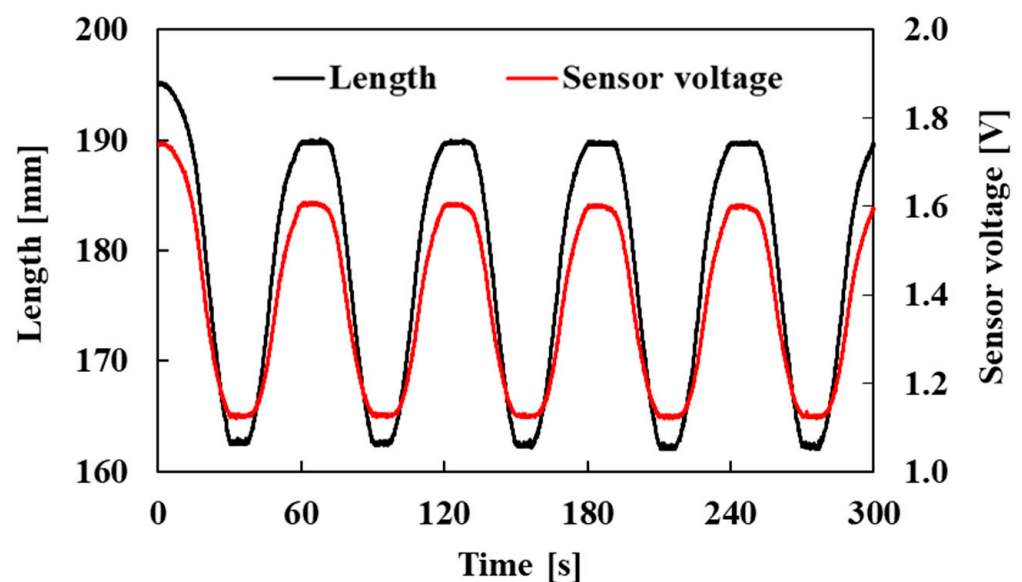


Figure 16. Length and sensor voltage variation with respect to time (pneumatic pressure: 0.0 MPa \rightarrow 0.3 MPa \rightarrow 0.0 MPa, five times).

Figure 16 shows the change in the sensor voltage and length; the red and black lines indicate these characteristics. As is evident, the sensor voltage followed the length without a phase shift.

The relationship between the length of the active string actuator and voltage output of the optical fiber sensor is shown in Figure 17. The relationship between the active string length and the sensor voltage followed the same route, so we consider the sensor output to be highly reproducible.

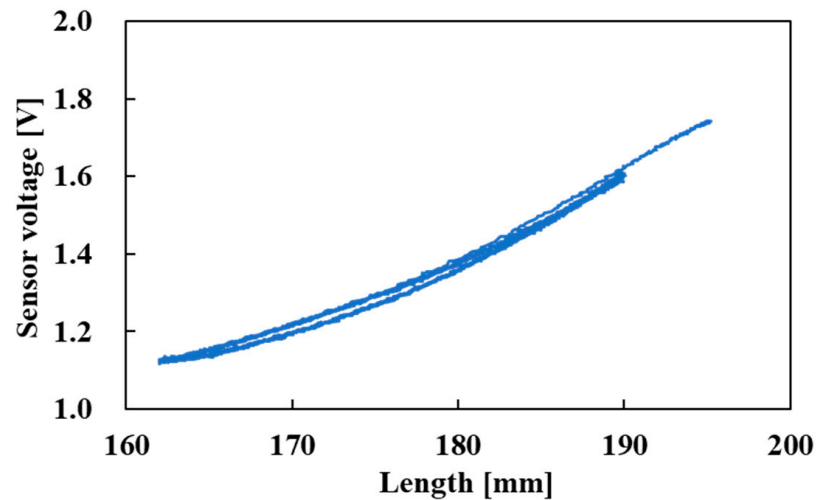


Figure 17. Relationship between length and sensor voltage (pneumatic pressure: 0.0 MPa \rightarrow 0.3 MPa \rightarrow 0.0 MPa, five times).

Furthermore, experiments were conducted in which loads of 2.0 N and 3.0 N were added to the actuator to examine the effect of load on the sensor characteristics. The condition for pneumatic pressure was the same as that in the experiment in Figure 16. Pneumatic pressure was repeatedly applied to the active string actuator with the optical fiber sensor five times, rising from 0.0 MPa to 0.3 MPa and falling back to 0.0 MPa. The measurement results are shown in Figure 18. The figure shows a comparison of three conditions, namely, loads of 1.0 N, 2.0 N, and 3.0 N.

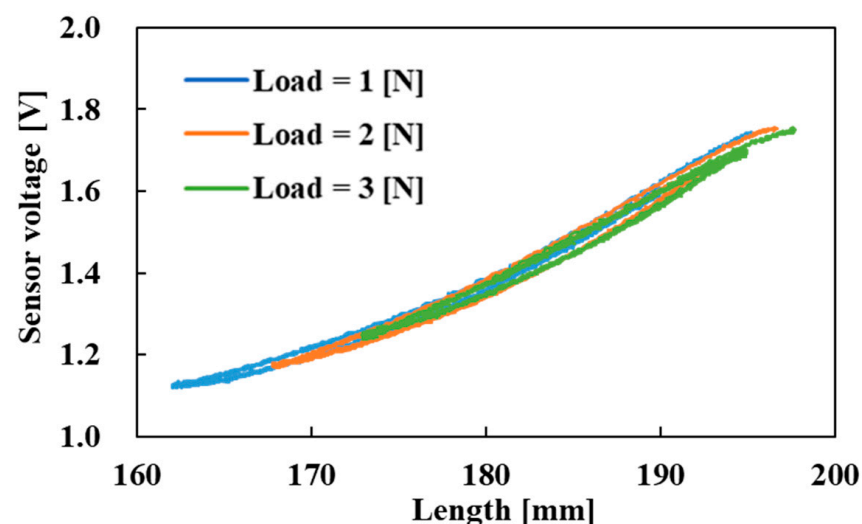


Figure 18. Change in sensor voltage due to load.

The driving range of the actuator (i.e., length range) depends on the load; therefore, the length range differs according to the load. However, it was found that the sensor voltage of each condition overlapped. This implies that the sensor output corresponds to the length of the active string actuator and does not depend on the load. The sensor voltage correlated with the length of the active string actuator in the entire driving range, and the relationship between the length L and the sensor voltage V_S derived from Figure 18 is approximated as

given below. Here, R^2 is the coefficient of determination of the approximate equation; a value of 0.993 demonstrates the high agreement of the equation.

$$L = -41.89V_S^2 + 170.7V_S + 24.95 \quad (2)$$

$$R^2 = 0.993.$$

The maximum error in the length between the measurement results and the approximate formula is 2.5 mm, which represents 7.6% of the driving range of the actuator. The optical fiber was not fixed to thin artificial muscles, so hysteresis occurred. Although currently the error may still be large, through this study, the voltage output of the optical fiber sensor was correlated with the length of the active string actuator, indicating the possibility of estimating the length of the active string actuator by using the optical fiber sensor.

4. Conclusions

In this study, we propose a new method for sensing the length of an active string actuator. We integrated a step-index multimode optical fiber in an active string actuator and used a photo IC diode to measure changes in the amount of light propagating in the optical fiber to estimate the length of the active string actuator. The step-index multimode optical fiber can be easily integrated in active string actuators in a wave-like pattern. Fundamental experiments were conducted, and the results are summarized below.

1. The integration of the optical fiber sensor reduced the contraction of the active string actuator by 1.5 mm, which is 4.5% of the contraction of the active string actuator without the optical fiber. This reduction owes to the stiffness of the optical fiber and friction between the fiber and the active string; however, the degree of reduction was small.
2. The sensor voltage acquired using the embedded optical fiber sensor changed with the length of the active string actuator. This suggests that it is possible to estimate the displacement of the active string actuator using the optical fiber sensor.

A thinner optical fiber with a low stiffness will be integrated in a future study to improve the reduction in the contraction characteristics, and the optimal composite pitch of the optical fiber will be determined. In addition, displacement control experiments will be conducted to demonstrate the usefulness of optical fiber sensor.

Although the effect of temperature was not investigated in this study, all of the experiments were carried out at room temperature (20 °C), and the sensor values were found to be stable. In the future, we would like to study the effect of temperature. In addition, the optical fiber contacted with thin artificial muscles, so the possibility of microbending losses cannot be ruled out. However, as the optical fiber was not fixed to thin artificial muscles, and there were gap spaces between the thin artificial muscles, when the active string contracted, the fiber escaped into the gap; therefore, high stress was not added to the fiber. In addition, thin artificial muscles had a very soft structure and the stress on the optical fiber was small. Therefore, the microbending losses are considered sufficiently small. In this study, the focus was on bending losses, but in future work, we would like to examine the influence of microbending losses using fiber Bragg grating (FBG).

Author Contributions: Conceptualization, W.T. and S.W.; methodology, W.T.; validation, W.T.; data curation, W.T.; writing—original draft preparation, W.T. and S.W.; writing—review and editing, S.W.; T.K. and D.Y.; funding acquisition, S.W. All authors have read and agreed to the published version of the manuscript.

Funding: This research was partially supported by Grants-in-Aid for Scientific Research (Grant Number 20K04240) by Japan Society for the Promotion of Science, and Grant for the Promotion of Science and Technology 2021 in Okayama Prefecture by The Ministry of Education, Culture, Sports, Science and Technology in Japan.

Institutional Review Board Statement: Not applicable.

Informed Consent Statement: Not applicable.

Data Availability Statement: Not applicable.

Conflicts of Interest: The authors declare no conflict of interest.

References

1. Gaylord, R.H. Fluid Actuated Motor System and Stroking Device. U.S. Patent 2-238-058, 22 July 1958.
2. DARWING Power Assist Glove EX. Available online: <https://www.daiyak.co.jp/product/detail/?id=907> (accessed on 22 March 2022).
3. Muscle Suit Every. Available online: <https://innophys.net/musclesuit> (accessed on 22 March 2022).
4. Kurumaya, S.; Nabae, H.; Endo, G.; Suzumori, K. Design of Thin McKibben Muscle and Multifilament Structure. *Sens. Actuators A Phys.* **2017**, *261*, 66–74. [[CrossRef](#)]
5. Kurumaya, S.; Nabae, H.; Endo, G.; Suzumori, K. Active Textile Braided in Three Strands with Thin McKibben Muscle. *Soft Robot.* **2019**, *6*, 250–262. [[CrossRef](#)] [[PubMed](#)]
6. Koizumi, S.; Kurumaya, S.; Nabae, H.; Endo, G.; Suzumori, K. Braiding Thin McKibben Muscles to Enhance Their Contracting Abilities. *IEEE Robot. Autom. Lett.* **2018**, *3*, 3240–3246. [[CrossRef](#)]
7. Abe, T.; Koizumi, S.; Nabae, H.; Endo, G.; Suzumori, K.; Sato, N.; Adachi, M.; Takamizawa, F. Fabrication of “18 Weave” Muscles and Their Application to Soft Power Support Suit for Upper Limbs Using Thin McKibben Muscle. *IEEE Robot. Autom. Lett.* **2019**, *4*, 2532–2538. [[CrossRef](#)]
8. Hiramitsu, T.; Suzumori, K.; Nabae, H.; Endo, G. Experimental Evaluation of Textile Mechanisms Made of Artificial Muscles. In Proceedings of the 2019 2nd IEEE International Conference on Soft Robotics (RoboSoft), Seoul, Korea, 14–18 April 2019. [[CrossRef](#)]
9. Koizumi, S.; Chang, T.; Nabae, H.; Endo, G.; Suzumori, K.; Mita, M.; Saitoh, K.; Hatakeyama, K.; Chida, S.; Shimada, Y. Soft Robotic Gloves with Thin McKibben Muscles for Hand Assist and Rehabilitation. In Proceedings of the 2020 IEEE/SICE International Symposium on System Integration (SII), Honolulu, HI, USA, 12–15 January 2020. [[CrossRef](#)]
10. Takada, M.; Wakimoto, S.; Oshikawa, T.; Ueda, T.; Kanda, T. Active Cloth Fabricated by a Flat String Machine and its Application to a Safe Wheelchair System. *J. Robot. Mechatron.* **2020**, *32*, 1010–1018. [[CrossRef](#)]
11. Abe, T.; Koizumi, S.; Nabae, H.; Endo, G.; Suzumori, K. Muscle Textile to Implement Soft Suit to Shift Balancing Posture of the Body. In Proceedings of the 2018 IEEE International Conference on Soft Robotics (RoboSoft), Livorno, Italy, 24–28 April 2018. [[CrossRef](#)]
12. Kurumaya, S.; Suzumori, K.; Nabae, H.; Wakimoto, S. Musculoskeletal Lower-Limb Robot Driven by Multifilament Muscles. *Robomech J.* **2016**, *3*, 18. [[CrossRef](#)]
13. Doi, T.; Wakimoto, S.; Suzumori, K.; Mori, K. Proposal of Flexible Robotic Arm with Thin McKibben Actuators Mimicking Octopus Arm Structure. In Proceedings of the 2016 IEEE/RSJ International Conference on Intelligent Robots and Systems (IROS), Daejeon, Korea, 9–14 October 2016. [[CrossRef](#)]
14. Tian, W.; Wakimoto, S.; Kanda, T.; Yamaguchi, D. Fabrication of “Active String” using Thin Artificial Muscles by String Production Process. In Proceedings of the Mechanical Engineering Congress (MECJ-21), Online, Japan, 5–8 September 2021. (In Japanese)
15. Wakimoto, S.; Suzumori, K.; Kanda, T. Development of Intelligent McKibben Actuator. In Proceedings of the IEEE/RSJ International Conference on Intelligent Robots and Systems, Seoul, Korea, 5–9 June 2005.
16. Park, Y.L.; Wood, R.J. Smart Pneumatic Artificial Muscle Actuator with Embedded Microfluidic Sensing. In Proceedings of the IEEE SENSORS 2013, Baltimore, MD, USA, 3–6 November 2013. [[CrossRef](#)]
17. Felt, W.; Chin, K.Y.; Remy, C.D. Contraction Sensing with Smart Braid McKibben Muscles. *IEEE/ASME Trans. Mechatron.* **2016**, *21*, 1201–1209. [[CrossRef](#)] [[PubMed](#)]
18. Legrand, J.; Loenders, B.; Vos, A.; Schoevaerdts, L.; Poorten, E.V. Integrated Capacitance Sensing for Miniature Artificial Muscle Actuators. *IEEE Sens. J.* **2020**, *20*, 1363–1372. [[CrossRef](#)]
19. Yano, T.; Fujimoto, S.; Akagi, T.; Kobayashi, W. Development of Outer Diameter Sensor for Position Control of McKibben Artificial Actuator Using Hall-Effect Sensor. *Int. J. Mech. Eng. Robot. Res.* **2020**, *9*, 190–196. [[CrossRef](#)]
20. Tiziani, L.O.; Hammond, F.L. Optical Sensor-Embedded Pneumatic Artificial Muscle for Position and Force Estimation. *Soft Robot.* **2020**, *7*, 462–477. [[CrossRef](#)] [[PubMed](#)]
21. Akagi, T.; Dohta, S.; Kenmotsu, Y.; Zhao, F.; Yoneda, M. Development of Smart Inner Diameter Sensor for Position Control of McKibben Artificial Muscle. *Procedia Eng.* **2012**, *41*, 105–112. [[CrossRef](#)]
22. Shimooka, S.; Dohta, S.; Akagi, T.; Moriwake, Y. Position Control of Rubber Artificial Muscle Using Built-in Ultrasonic Sensor and Quasi-Servo Valve. *Int. J. Mech. Eng. Robot. Res.* **2015**, *4*, 304–308. [[CrossRef](#)]
23. Schulte, H.F. The Characteristics of the McKibben Artificial Muscle. In *The Application of External Power in Prosthetics and Orthotics*; National Academy of Sciences; National Research Council: Washington, DC, USA, 1961; pp. 94–115.
24. Nakamura, T. *Illustration Artificial Muscles—The World Opened Up by Soft Actuators*, 1st ed.; The Nikkan Kogyo Shimbun: Tokyo, Japan, 2011; pp. 56–61. (In Japanese)
25. Tian, W.; Wakimoto, S.; Nagaoka, K.; Yoshimoto, Y.; Kanda, T.; Yamaguchi, D. Displacement Sensing of an Active String Actuator by an Optical Fiber. *Eng. Proc.* **2021**, *10*, 35. [[CrossRef](#)]